Thermochimica Acta 489 (2009) 63–69

Contents lists available at ScienceDirect

Thermochimica Acta

journal homepage: www.elsevier.com/locate/tca

Thermal analysis of azoic dyes: Part I. Non-isothermal decomposition kinetics of [4-(4-chlorobenzyloxy)-3-methylphenyl](*p*-tolyl)diazene in dynamic air atmosphere

A. Rotaru[a,*], G. Brătulescu[b], P. Rotaru[c]

[a] *Inflpr – National Institute for Laser, Plasma and Radiation Physics, Lasers Department, Bvd. Atomistilor, Nr. 409, PO Box MG-16, RO-077125 Magurele, Bucharest, Romania*
[b] *University of Craiova, Faculty of Chemistry, Calea Bucuresti Str., Nr. 107 I, Craiova, Romania*
[c] *University of Craiova, Faculty of Physics, A.I. Cuza Str., Nr. 13, Craiova, Romania*

ARTICLE INFO

Article history:
Received 18 August 2008
Received in revised form 16 January 2009
Accepted 19 January 2009
Available online 30 January 2009

Keywords:
Azomonoether dyes
"Mode-free" kinetics
IKP method
Perez-Maqueda et al. criterion
Master plot procedure

ABSTRACT

Thermal analysis of [4-(4-chlorobenzyloxy)-3-methylphenyl](*p*-tolyl)diazene dye, was performed in dynamic air atmosphere. The compound behavior was investigated using TG, DTG, DTA and DSC techniques, under non-isothermal linear regime. Kinetic parameters of the two decomposition steps were evaluated by means of multi-heating rates methods, such as "mode-free" kinetic methods, IKP method, Perez-Maqueda et al. criterion and Master plot procedure. It was shown that the conversion function which describes the process it is not necessary one of the best-fitting functions (when using single-heating rate methods). IKP method can however reduce the possibilities of choosing the true function which can be precisely obtained by applying discrimination methods.

1. Introduction

Thermal analysis and kinetic studies of thermal-induced changes of new compounds designed for temperature controlled applications (like dyes exhibiting liquid-crystalline nature) are a real need and an advantageous pointer before trying to functionalize them [1–6]. From the point of view of possible applications (*e.g.* liquid crystals for non-linear optics applications, for dye lasers, plastic composite materials or textiles industry) [7–9], azomonoethers are a large interest class of dyes. Part I on the thermal analysis of azomonoether dyes, aims to identify the physical and chemical transformations of [4-(4-chlorobenzyloxy)-3-methylphenyl](*p*-tolyl)diazene [10], related to non-isothermal increasing temperature regimes in dynamic air atmosphere and to establish the kinetic parameters of the observed decomposition steps.

A cause of materials' aspect and color modifications is due to the thermal-induced chemical degradation of organic dye used. The present studied compound [4-(4-chlorobenzyloxy)-3-methylphenyl](*p*-tolyl)diazene is one of the new potential category of organic azoeteric dyes for the plastic materials and textiles industries, having a high chemical stability. In order to establish the thermochemical stability domain and in general the limits of such dyes use, it is necessary to study the their thermal behavior and follow the thermo-oxidative processes. Not only the temperature limits of use are important, but also the technological process of materials (that contain them) fabrication is very important to be followed since higher temperatures may be employed. Apart from the used temperature regime in the technological processing of new materials, the knowledge of kinetic parameters is very important as universal characteristic of this process. Therefore, predictions of thermal behaviors of a certain dye may be made in other temperature conditions, experimentally undone. For example, for small heating rates or isothermal regimes at low temperatures, the degradation may begin at lower temperatures as known. Judging this way, one may provide clues to those deciding the use of a certain dye or of another, as well as the possibility of predicting the appropriate temperature regime needed in the technological process; choosing a compound that little decomposes (for example 2–3%) at a certain temperature – insufficient for deteriorating the finite material – instead of another that does not decompose, but effectively costs much more when obtained.

In the case of dye lasers, the problem may be reverse judged; the lifetime of the dyes under laser constant irradiation parameters, the decomposed dye percentage and the kinetic parameters may be used for a kind of average apparent temperature profile estimation.

Recent papers have reported on the critical analysis of the single heating-rate model-fitting methods [11–14], suggesting that their

* Corresponding author. Tel.: +40 745379205.
E-mail address: andrei.rotaru@inflpr.ro (A. Rotaru).

0040-6031/$ – see front matter © 2009 Elsevier B.V. All rights reserved.
doi:10.1016/j.tca.2009.01.023

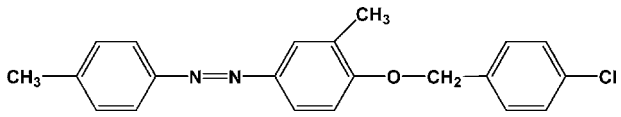

Fig. 1. [4-(4-Chlorobenzyloxy)-3-methylphenyl](*p*-tolyl)diazene.

use would lead to uncertain and even wrong values of the activation parameters. To evaluate the entire kinetic triplet that describes a physical or chemical transformation, more sophisticated kinetic methods like Invariant Kinetic Parameters method [15] (to determinate the pre-exponential factor) and Perez-Maqueda et al. criterion [16] or Master plot procedure [17,18] (to find the right conversion function) were used. Besides the kinetic evaluation, this paper aims to be a guide for manipulating the existing kinetic methods, but also to bring to the public the way of kinetic models' correlations.

2. Experimental

The obtaining of [4-(4-chlorobenzyloxy)-3-methylphenyl](*p*-tolyl)diazene was made by microwave assisted condensation reaction of 4-chlorobenzyl chloride with 4-hydroxy-3,4′-dimethylazobenzene in alkaline medium under organic solvent-free conditions (Williamson azoether synthesis) [10], no inorganic support being necessary since one of the reagents presents a polar structure and plays the role of an absorbent. A Bauknecht microwave apparatus was employed for the synthesis, using the following parameters: $P = 650$ W, $\lambda = 12.2$ cm, $t = 170$ s and $\eta > 99\%$ was obtained. Thermal analysis measurements (TG, DTG, DTA and DSC) on the investigated compound (Fig. 1) were carried out in dynamic air atmosphere (150 mL min^{-1}), under non-isothermal linear conditions. A horizontal Diamond differential/thermogravimetric analyzer from PerkinElmer Instruments was used during the experiments.

Samples from 0.8 to 1.5 mg, contained in Al_2O_3 crucibles, were heated in the temperature range 20–700 °C, with the heating rates of: 2, 4 and 10 K min^{-1}.

3. Results and discussion

3.1. Thermal analysis

Fig. 2 shows the thermoanalytical curves (TG, DTG, DTA and DSC) of [4-(4-chlorobenzyloxy)-3-methylphenyl](*p*-tolyl)diazene, recorded for 10 K min^{-1}; similar curves were obtained for all other heating rates.

After melting at 131.5 °C, in the 270–330 °C temperature range, the investigated compound undergoes an oxidative decomposition. A series of papers on the thermal analysis of such compounds revealed their different behaviors in air [19,20,41] and inert [6,21] dynamic atmospheres. The experimental weight of the remaining matter after the first step ($\Delta m_{exp} \approx 25\%$) is in good agreement with one of tropylium ion (stable at such high temperatures [22,23]) and tropylium-based residues formation ($\Delta m_{theor} = 25.9\%$). The combustion of residues (second step—TG curve) takes place between 468 and 597 °C.

DSC parameters for the thermal analysis of [4-(4-chlorobenzyloxy)-3-methylphenyl](*p*-tolyl)diazene at 10 K min^{-1} in dynamic air atmosphere are presented in Table 1.

3.2. Kinetic analysis

Budrugeac [24] reviewed a number of recent publications in the field, analyzed the procedural errors in the kinetic triplet {*E*, *A*, $f(\alpha)$} evaluation and proposed a general algorithm to be applied, straightforwardly the kinetic analysis must begin with the evaluation of the activation energy dependence on the conversion degree. The influence of different temperature regimes upon the thermal behavior of the investigated compounds can provide kinetic param-

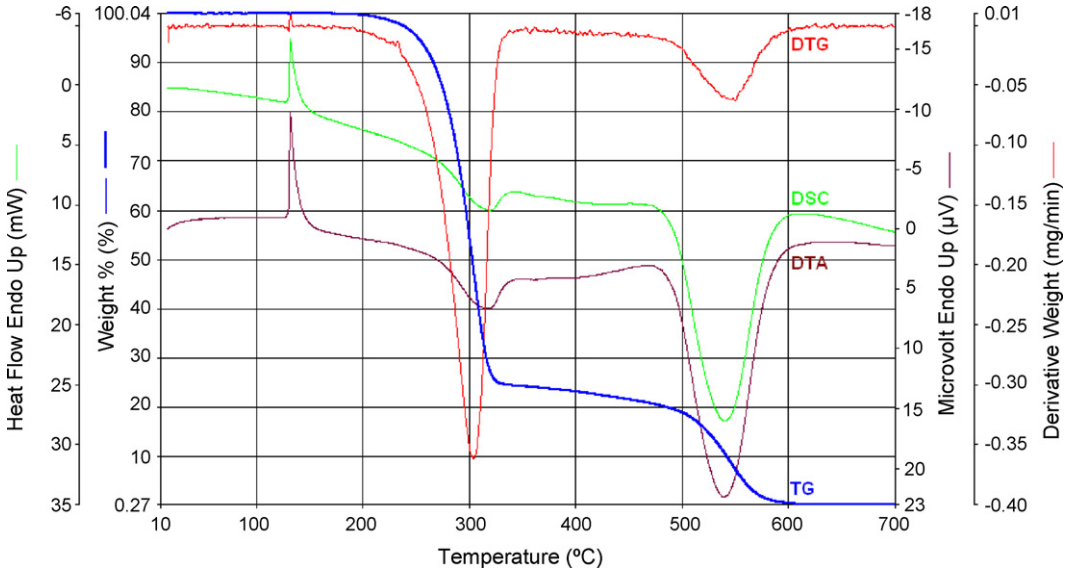

Fig. 2. Thermoanalytical curves of [4-(4-chlorobenzyloxy)-3-methylphenyl](*p*-tolyl)diazene at 10 K min^{-1} in dynamic air atmosphere.

Table 1
DSC parameters for [4-(4-chlorobenzyloxy)-3-methylphenyl](*p*-tolyl)diazene decomposition at $\beta = 10$ K min^{-1}.

Change	Thermal effect *Endo*/*exo*	Change temp. range/°C	Temp. of the max. change T_{max}/°C	Transferred heat ΔH/kJ kg^{-1}
Melting	Endothermic	127–150	131.5	111.7
Oxidative decomposition	Exothermic	270–330	306.3	−342.2
Combustion of residues	Exothermic	468–597	524.2	−4798.4

eters indicating change in the reaction pathway and thus a more complex process. When E does not depend on α, only a single reaction is involved, a unique kinetic triplet being expected to describe it. If E changes with α, then the process is complex. Vyazovkin and Lesnikovich [25] and then Vyazovkin [26] established an algorithm to identify the type of complex processes. When E increases with conversion degree, the process involves parallel reactions. When E decreases and the shape of its evolution is concave, then the process has reversible stages. For decreasing convex shape, the process changes the limiting stage.

Since from isoconversional methods the pre-exponential factor and conversion function cannot be determined in the same time, advanced methods have been developed. If the isoconversional activation energy remains constant, no variation of the pre-exponential factor should be encountered. Thus, the invariant activation parameters may be obtained by relating the apparent activation parameters to the compensation effect formalism [15]. Furthermore, by applying discrimination criteria between the conversion functions, the right reaction mechanism is to be found [16–18].

3.2.1. Isoconversional methods

The isoconversional ("model-free" kinetic) procedures are the most utilized methods to evaluate the activation energy of thermal-induced processes, to quote only a few recent papers in this journal [27–31] from at least 800 citations to be found on a simple search on the ISI Web of Knowledge database. They may be classified as linear (when the activation energy is evaluated from the slope of a straight line) and non-linear (when the activation energy is evaluated from a specific minimum condition).

In this paper we make use of Kissinger–Akahira–Sunose (KAS method)-integral linear method [32,33], Eq. (1)

$$\ln\frac{\beta}{T^2} = \ln\frac{A\cdot R}{E\cdot g(\alpha)} - \frac{E}{R\cdot T} \quad (1)$$

and of Flynn–Wall–Ozawa (FWO method)-integral linear method [34,35], Eq. (2)

$$\ln\beta = \ln\frac{A\cdot E}{R\cdot g(\alpha)} - 5.331 - 1.052\frac{E}{R\cdot T} \quad (2)$$

where α is the conversion degree, A is the pre-exponential factor, E is the activation energy, $g(\alpha)$ is the integral conversion function and R is the universal gas constant.

Thus, for α = const., the plot $\ln(\beta/T^2)$ *vs.* $(1/T)$ or $\ln(\beta)$ *vs.* $(1/T)$, obtained from the experimental thermogravimetric curves recorded for several constant-heating rates, should be a straight line, the activation energy being evaluated from these slopes.

Fig. 3 shows the results obtained using KAS and FWO methods, as values of the activation energy at various conversion degrees from 0.2 to 0.8 with a step of 0.01, both profiles totally overlapping.

The activation energy of the first decomposition step is constant, describing a single reaction. The accuracy in determining the activation energy by means of integral isoconversional methods is very high, the correlation coefficients being over 0.99750 (Fig. 4).

The mean values of the activation energy corresponding to the first thermal decomposition step, for α between 0.2 and 0.8 are

$$\bar{E}_{KAS} = 176.6 \pm 0.5\ \text{kJ mol}^{-1} \quad \bar{E}_{FWO} = 176.5 \pm 0.6\ \text{kJ mol}^{-1}$$

The second thermal decomposing step (combustion of tropyliu or tropylium-based residues) is characterized by decreasing isoconversional activation energy (Fig. 5).

The isoconversional activation energy of the second decomposition step decreases from 170 to 145 kJ mol^{-1} with the consumption of the reaction, by the correlation coefficients in Fig. 6.

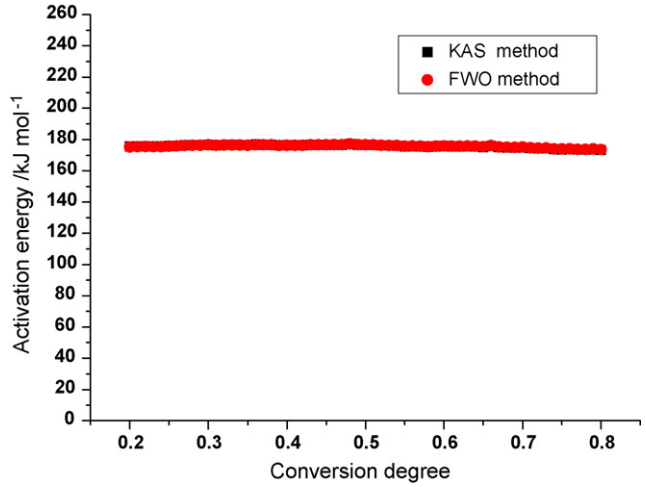

Fig. 3. Isoconversional activation energy of the linear non-isothermal decomposition of [4-(4-chlorobenzyloxy)-3-methylphenyl](*p*-tolyl)diazene in dynamic air atmosphere (first step).

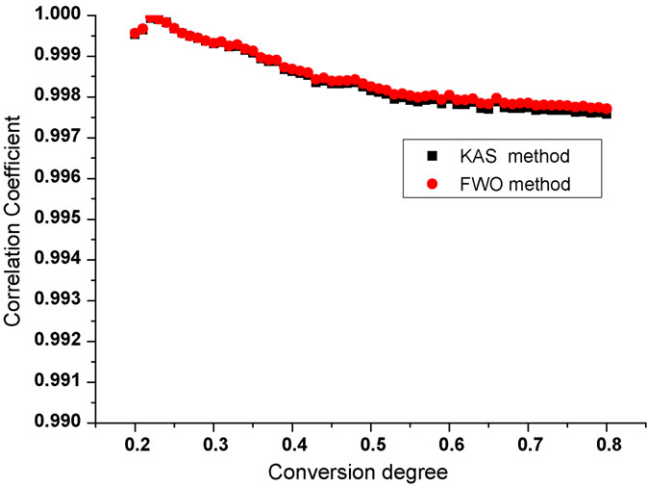

Fig. 4. Correlation coefficients for the isoconversional activation energy evaluation of the thermal decomposition of [4-(4-chlorobenzyloxy)-3-methylphenyl](*p*-tolyl)diazene (first step).

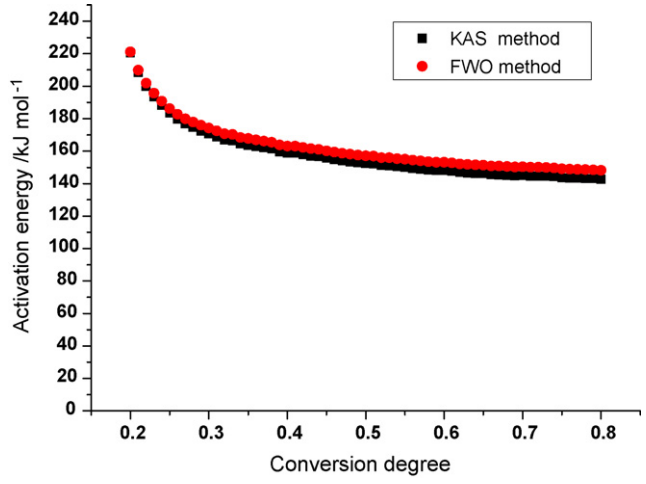

Fig. 5. Isoconversional activation energy corresponding to the linear non-isothermal combustion in dynamic air atmosphere of the residues (second step).

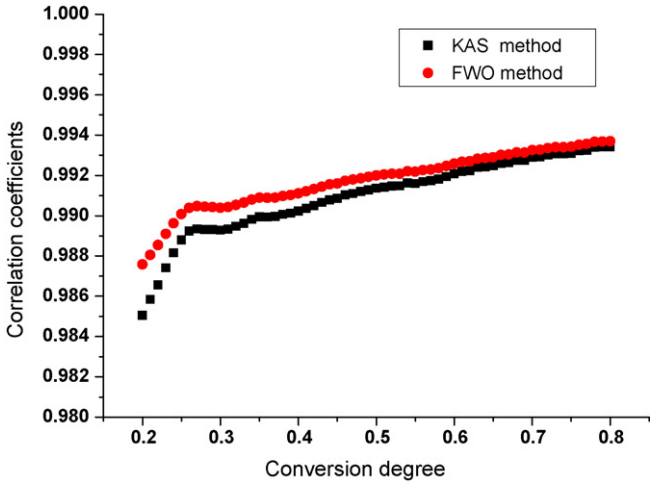

Fig. 6. Correlation coefficients for the isoconversional activation energy evaluation of the linear non-isothermal combustion in dynamic air atmosphere of the residues (second step).

3.2.2. Invariant kinetic parameters (IKP) method

Criado and Morales observed [36] that almost any $\alpha = \alpha(T)$ or $(d\alpha/dt) = (d\alpha/dt)(T)$ experimental curve may be correctly described by several conversion functions when an integral or differential model-fitting method is used. Although the values are obtained with high accuracy, they change with different heating rates and among the conversion functions that were used. These values are known as apparent activation parameters.

For evaluating the apparent activation parameters of the first decomposition step, we have chosen as model-fitting method that one derived by Coats and Redfern [37]; for each heating rate, the best-fitting kinetic models results are presented in Table 2.

In order to obtain the invariant (true) activation parameters (E_{inv}, A_{inv}), the apparent activation energies and the logarithms of apparent pre-exponential factors corresponding to each heating rate must be gathered under the compensation effect rule (Eq. (3)), as it has been suggested by Lesnikovich and Levchik [15].

$$\ln A = a_\beta + b_\beta \cdot E \tag{3}$$

The plot of apparent kinetic parameters corresponding to the thermal decomposition in air flow of [4-(4-chlorobenzyloxy)-3-methylphenyl](*p*-tolyl)diazene are represented (Fig. 7a).

As these heating rate-dependent straight lines intersect in a region (area delimited by the circle in the detailed image of apparent kinetic parameters plot, Fig. 7b) rather than in the isoparametric point [38], the invariant kinetic parameters cannot be determined using only this approach.

Only the compensation effect parameters (a_β, b_β) obtained for several constant heating rates, plotted according to the super-correlation equation (Eq. (4)), may lead to the invariant kinetic parameters (E_{inv}, A_{inv}).

$$a_\beta = \ln A_{inv} - b_\beta \cdot E_{inv} \tag{4}$$

It is easily to notice from Fig. 7 that low Fn conversion functions (for $n = 0.3–0.6$) are not the most adequate, because the intersection is around 175 ± 20 kJ mol^{-1} (Fig. 7b). Even if the correct conversion function cannot be precisely determined by IKP method, it might offer precious clues, restricting the possibilities to those functions in-between the intersection region; in this case, it should correspond to middle-range reaction order functions (Fn where $n = 1–2$). Despite D2 model provided apparent activation parameters with high correlation coefficients, it was previously shown [39,40] that in such cases (liquid state decomposition), the contribution of diffusion functions is less probable, they even providing increased errors.

For several groups of apparent activation parameters listed in Table 2, obtained by different kinetic models (all kinetic models: AKM = {F0.3; F0.35; F0.4; F0.45; F0.5; F0.55; A0.1; D2}), we tried to establish the best combination ($r \to 1$), a better resolution in determining the invariant kinetic parameters and the closest value to the mean isoconversional activation energies [40–43] (Table 3).

The correlation coefficients in Table 3 show a good agreement of all kinetic models, less D2 model. All combinations of kinetic models provide high accuracy compensation effect parameters (a_β, b_β). The elimination of only A0.1 kinetic model leads to wrong results which can be observed as well in Table 4, this combination should be excluded right from the start. Keeping D2 function (comparing with AKM-{D2;A0.1}) and removing only A0.1, deviates the straight line to its wrong values, decreasing the correlation coefficient.

Comparing to AKM model (Fig. 8a), the plot of a_β *vs.* b_β for AKM-{D2;A0.1} has the highest correlation coefficient ($r = 1$) and is a true straight line (Fig. 8b). Depending on the chosen group of kinetic models, the compensation effect parameters are obtained with different accuracies, their values and derived invariant activation parameters varying substantially. A short look in Table 3 makes compulsory the exclusion of mechanism D2, but until here, the elimination of A0.1 is not compulsory. The efficiency of IKP method is strongly revealed by AKM-{D2;A0.1} and even by AKM which comprises all the best-fitting functions that makes it a more powerful method. From Table 4 it results that A0.1 must be eliminated only together with D2.

As it was expected, the best results for invariant kinetic parameters determination were obtained by AKM-{D2;A0.1}, AKM and AKM-{D2} in this order. For these three groups, the invariant activation energy is around 174–178 kJ mol^{-1}, close to 176.6 kJ mol^{-1} obtained by KAS method and 176.5 kJ mol^{-1} by FWO method. For AKM-{D2;A0.1}, the invariant kinetic parameters are $E_{inv} = 178.0$ kJ mol^{-1} and $\ln A_{inv} = 33.208$ ($A = 2.4\ 10^{14}$ s^{-1}), obtained with $r = 0.99999$.

Table 2
Apparent activation parameters by Coats–Redfern equation for each constant-heating rate.

Kinetic model	$\beta = 2$ K min^{-1}			$\beta = 4$ K min^{-1}			$\beta = 10$ K min^{-1}		
	E/kJ mol^{-1}	ln A, A/s^{-1}	r	E/kJ mol^{-1}	ln A, A/s^{-1}	r	E/kJ mol^{-1}	ln A, A/s^{-1}	r
F0.3	114.2	18.084	0.99994	109.9	17.335	0.99996	112.8	18.317	0.99985
F0.35	116.3	18.600	0.99996	112.0	17.829	0.99997	114.9	18.811	0.99991
F0.4	118.5	19.123	0.99995	114.2	18.328	0.99995	117.1	19.312	0.99996
F0.45	120.8	19.653	0.99991	116.3	18.835	0.99991	119.3	19.820	0.99997
F0.5	123.0	20.191	0.99985	118.5	19.340	0.99984	121.6	20.335	0.99996
F0.55	125.4	20.737	0.99977	120.8	19.866	0.99975	123.9	20.858	0.99992
F0.6	127.7	21.290	0.99966	123.0	20.388	0.99963	126.2	21.388	0.99986
D2	239.0	45.048	0.99995	230.7	42.915	0.99996	236.6	43.961	0.99987
A0.1	1558.6	336.18	0.99818	1506.8	319.325	0.99811	1546.2	321.295	0.99870

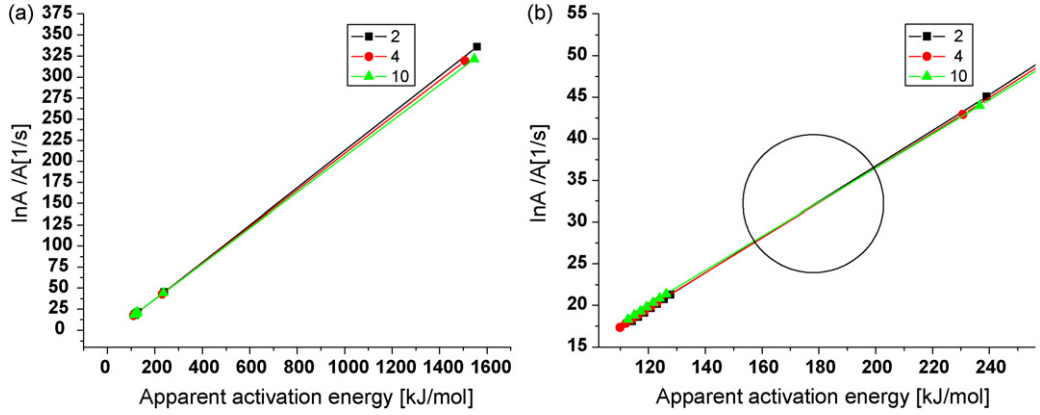

Fig. 7. (a) Compensation effect for all best fitting kinetic models in the ln*A vs. E* space (first step) and (b) details of compensation effect for all best fitting kinetic models in the ln*A vs. E* space (first step).

Table 3
Compensation effect parameters for several combinations of kinetic models.

β/K min^{-1}	AKM			AKM-{A0.1}		
	a_β, A/s^{-1}	b_β/mol J^{-1}	r	a_β, A/s^{-1}	b_β/mol J^{-1}	r
2	−7.01601 ± 0.09448	$2.2017 \times 10^{-4} \pm 1.7616 \times 10^{-7}$	1	−6.32754 ± 0.13512	$2.1505 \times 10^{-4} \pm 9.5684 \times 10^{-7}$	0.99994
4	−6.39207 ± 0.09381	$2.1613 \times 10^{-4} \pm 1.8096 \times 10^{-7}$	1	−5.71066 ± 0.13388	$2.1088 \times 10^{-4} \pm 9.8342 \times 10^{-7}$	0.99993
10	−5.4767 ± 0.09416	$2.1131 \times 10^{-4} \pm 1.7700 \times 10^{-7}$	1	−4.79377 ± 0.13564	$2.0618 \times 10^{-4} \pm 9.7143 \times 10^{-7}$	0.99993

β/K min^{-1}	AKM-{D2}			AKM-{D2;A0.1}		
	a_β, A/s^{-1}	b_β/mol J^{-1}	r	a_β, A/s^{-1}	b_β/mol J^{-1}	r
2	−6.94018 ± 0.03384	$2.2015 \times 10^{-4} \pm 6.0154 \times 10^{-8}$	1	−8.94531 ± 0.01008	$2.3674 \times 10^{-4} \pm 8.3381 \times 10^{-8}$	1
4	−6.31676 ± 0.03364	$2.1611 \times 10^{-4} \pm 6.1865 \times 10^{-8}$	1	−8.30262 ± 0.03321	$2.3317 \times 10^{-4} \pm 2.8502 \times 10^{-7}$	1
10	−5.4012 ± 0.03415	$2.1129 \times 10^{-4} \pm 6.1199 \times 10^{-8}$	1	−7.41372 ± 0.01010	$2.2814 \times 10^{-4} \pm 8.4509 \times 10^{-7}$	1

Table 4
Invariant kinetic parameters for several combinations of kinetic models.

Kinetic models	E_{inv}/kJ mol^{-1}	ln A_{inv}, A_{inv}/s^{-1}	r
AKM	174.3 ± 10.0	32.325 ± 2.170	0.99834
AKM-{A0.1}	173.2 ± 13.5	30.897 ± 2.858	0.99695
AKM-{D2}	174.2 ± 10.1	31.394 ± 2.183	0.99832
AKM-{A0.1;D2}	178.0 ± 0.9	33.208 ± 0.209	0.99999

3.2.3. *Perez-Maqueda et al. criterion and Master plot procedure*

The process description is not complete without identifying the entire kinetic triplet and therefore the conversion function that describes the mechanism of reaction. Most frequently, the correct conversion function is to be found in the group of functions employed by IKP method, although this method is not able to establish the true function, but usually only restricts the possibilities of probable mechanisms (*i.e.* all possibilities of Fn type models, with $n = 0.3–0.6$). However, in our case, the true conversion function must be searched between the middle-range reaction order mechanisms (Fig. 7b).

In order to obtain the appropriate kinetic model of the first decomposition step, one can discriminate between the set of conversion functions by applying the Perez-Maqueda et al. criterion [16] or Master plot procedure [17,18], which were previously used with good outcomes by several authors [44–48].

According to Perez-Maqueda et al. criterion, the correct kinetic model corresponds to the independence of the activation param-

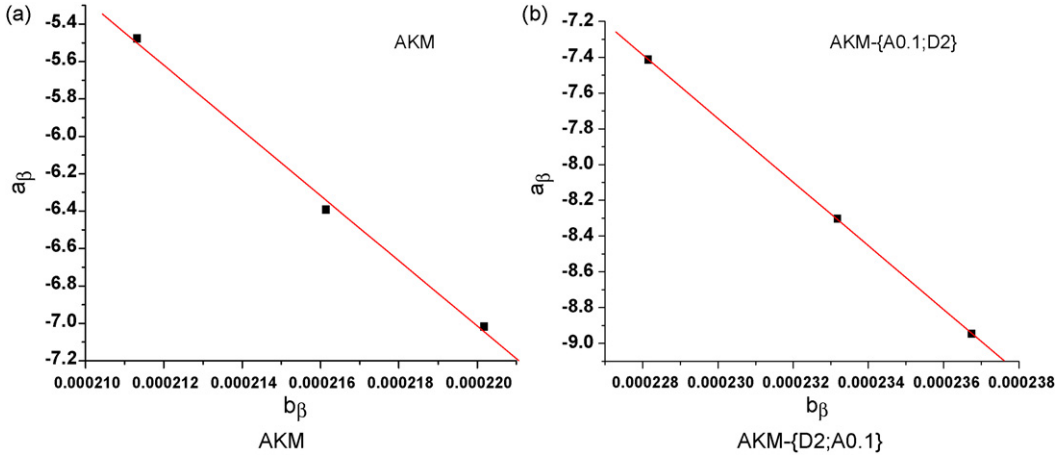

Fig. 8. Supercorrelation (compensation effect parameters) plot for the best two combination of kinetic models (first step).

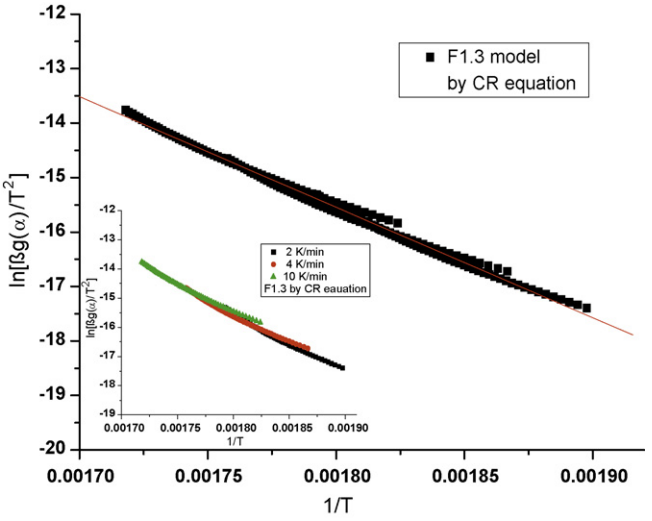

Fig. 9. Perez-Maqueda et al. straight lines for 2, 4 and 10 K min^{-1} dynamic air atmosphere decomposition of [4-(4-chlorobenzyloxy)-3-methylphenyl](*p*-tolyl)diazene (first step).

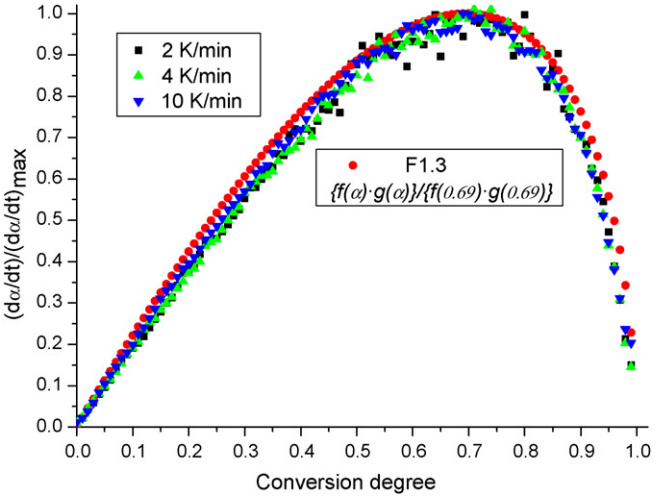

Fig. 10. Master plot procedure applied for 2, 4 and 10 K min^{-1} dynamic air atmosphere decomposition of [4-(4-chlorobenzyloxy)-3-methylphenyl](*p*-tolyl)diazene (first step).

eters on the heating rate. By applying any differential or integral model-fitting method, for every constant heating rate, the true kinetic model shall provide both the same constant activation energy as well as the pre-exponential factor. If the Coats–Redfern equation rewritten in the form

$$\ln\frac{\beta g(\alpha)}{T^2} = \ln\frac{AR}{E} - \frac{E}{RT} \tag{5}$$

is used, for the correct conversion function, all the points $\{\ln[\beta g(\alpha)/T^2]$ *vs.* $1/T\}$ corresponding to all applied heating rates lie on the same straight line (Fig. 9).

For F1.3 kinetic model, the best overlapping of the $\{\ln[\beta g(\alpha)/T^2]$ *vs.* $1/T\}$ points corresponding to the different heating rates was obtained, resulting the following kinetic parameters ($r = 0.99714$):

$$E = 169.7 \pm 3.1\ \text{kJ mol}^{-1} \qquad \ln A = 30.91 \pm 5.2\ (A/\text{s}^{-1})$$

$$A = 2.5 \times 1013 \pm 1.8 \times 10^2\ \text{s}^{-1}$$

However, because of inherent errors, detailed image in Fig. 9 indicates a incomplete overlapping of $\{\ln[\beta g(\alpha)/T^2]$ *vs.* $1/T\}$ points for all three constant-heating rates (2, 4, 10 K min^{-1}) employed, especially at low and high conversion. This is the cause of the difference between isoconversional or IKP results ($E \sim 178$ kJ mol^{-1}) and Perez-Maqueda et al. results ($E \sim 170$ kJ mol^{-1}) on the other hand.

To have a superior understanding on the true kinetic model, it is recommended to apply Master plot procedure [17,18]. When the problem of heating-rate dependency arises, the kinetic model is evaluated for each heating rate experiment. This procedure considers each thermal experiment independent of other ones.

Each conversion function has a precise shape and maximum of the reaction rate. By plotting the normalized reaction rate $([d\alpha/dt]/[d\alpha/dt]_{\max})$ *vs. conversion degree* of each constant heating-rate experiment, and comparing it to the normalized product of differential and integral conversion functions, the true kinetic model may be found.

In our case, as can be seen from Fig. 10, all normalized reaction rates completely overlap and are described by only one kinetic model: F1.3.

This criterion is the most powerful in identifying the true conversion function because it does not make any assumption on how the experimental data should behave.

Although F1.3 model belongs to the empirical expression of the conversion function suggested by Šesták and Berggren [49], it was found frequently describing thermal-induced decompositions of liquid systems.

However, the first decomposition step influences the formation of the residues and their decomposition; comparing with thermal decomposition of 2-allyl-4-((4-(4-methylbenzyloxy)phenyl)-diazenyl)phenol [23], where for the first step $\bar{E}_{KAS}$ is much lower (92.7 kJ mol^{-1}) than in this case (176.6 kJ mol^{-1}), other molecules forming each time. The difference in activation energies may explain the obtaining of some raw product (percentages indicating toluene or better at such temperatures the tropylium ions), but instead, the formation of different residues (based on tropylium fragments). Higher values of the activation energies induce the formation of better assembled molecules. Stronger bonds develop higher activation energies (at $\alpha = 0.5$, 150 kJ mol^{-1} in this case instead of 117 kJ mol^{-1}) for the combustion of the tropylium-based residues. Even if the decreasing dependencies of E_α on α are the same (concave) implying reversible reactions (equilibrium between various tropylium-based macromolecules), the two curves are of different values, but almost equidistant one to the other, suggesting the same type of chemical decomposition behavior.

4. Conclusions

Thermal analysis of [4-(4-chlorobenzyloxy)-3-methylphenyl]-(*p*-tolyl)diazene dye, was performed in dynamic air atmosphere. After melting at 131.5 °C, it undergoes an oxidative decomposition between 270 and 330 °C, followed by the combustion of residues from 468 to 597 °C. The activation energy of both decomposition steps were evaluated by means of multiple constant-heating rates methods, such as isoconversional (KAS and FWO) methods and since the isoconversional activation energy of the first decomposition step remains constant, it was possible to calculate its pre-exponential factor by means of IKP method as well. Gathering different kinetic models leads finally to invariant kinetic parameters in the region of middle-range reaction order models, and close to the isoconversional activation energies ($\sim 178 \pm 1$ kJ mol^{-1}). Perez-Maqueda et al. criterion and Master plot procedure were used in order to identify the true kinetic model that describes the oxidative decomposition of [4-(4-chlorobenzyloxy)-3-methylphenyl](*p*-tolyl)diazene. The supposition that the true conversion function should be one of the best-fitting functions was found to be incorrect. IKP method strongly restricts only the possibilities (when using single-heating rate methods), offering

indications and is sustained by the discrimination criteria. The use of Perez-Maqueda et al. criterion provided a 10^{13} order pre-exponential factor, close to the invariant pre-exponential factor (10^{14}) and when compared with the kinetic model obtained by Master plot procedure, F1.3 was indubitably established as the unique and right kinetic model. Comparing the activation energies for the pyrolysis of various types of tropylium ion-based residues, one have obtained information on bonding strength.

The paper finally provides the kinetic parameters of the thermo-oxidative process, needed by plastic composite materials, textile and lasers with dyes industries. The theoretical purpose is also accomplished, as being a supplementary guide for manipulating the existing kinetic methods, but also to bring to the public the way of kinetic models' correlations.

References

[1] M. Gűr, H. Kocaokutgen, M. Taş, Dyes Pigments 72 (2007) 101–108.
[2] M. Badea, A. Emandi, D. Marinescu, E. Cristurean, R. Olar, A. Braileanu, P. Budrugeac, E. Segal, J. Therm. Anal. Calorim. 72 (2003) 525–531.
[3] H. Dincalp, F. Toker, J. Durucasu, N. Avcibasi, S. Icli, Dyes Pigments 75 (2007) 11–24.
[4] A. Rotaru, A. Moanta, I. Salageanu, P. Budrugeac, E. Segal, J. Therm. Anal. Calorim. 87 (2007) 395–400.
[5] Z. Chen, Y. Wu, D. Gu, F. Gan, Dyes Pigments 76 (2008) 624–631.
[6] A. Rotaru, C. Constantinescu, P. Rotaru, A. Moanta, M. Dumitru, M. Dinescu, E. Segal, J. Therm. Anal. Calorim. 92 (2008) 279–284.
[7] T.-Y. Chao, H.-L. Chang, W.-C. Su, J.-Y. Wu, R.-J. Jeng, Dyes Pigments 77 (2008) 515–524.
[8] M. Lu, B.T. Cunningham, S.J. Park, J.G. Eden, Opt. Commun. 281 (2008) 3159–3162.
[9] A.M.F. Oliveira-Campos, M.J. Oliveira, L.M. Rodrigues, M.M. Silva, M.J. Smith, Thermochim. Acta 453 (2007) 52–56.
[10] G. Bratulescu, Y. Le Bigot, M. Delmas, Synthetic Commun. 27 (1997) 1037–1042.
[11] M. Maciejewski, S. Vyazovkin, Thermochim. Acta 370 (2001) 149–154.
[12] M.E. Brown, M. Maciejewski, S. Vyazovkin, R. Nomen, J. Sempere, A.K. Burnham, J. Opfermann, R. Strey, H. Andreson, A. Kemmler, R. Keuleers, J. Jannsens, H.O. Desseyn, C.R. Li, T.B. Tang, B. Roduit, J. Malek, T. Mitsuhasni, Thermochim. Acta 355 (2000) 125–143.
[13] B. Roduit, Thermochim. Acta 355 (2000) 171–180.
[14] S. Vyazovkin, J. Therm. Anal. Calorim. 83 (2006) 45–51.
[15] A.I. Lesnikovich, S.V. Levchik, J. Therm. Anal. 27 (1983) 89–94.
[16] L.A. Perez-Maqueda, J.M. Criado, F.J. Gotor, J. Malek, J. Phys. Chem. A 106 (2002) 2862–2868.
[17] J.M. Criado, L.A. Perez-Maqueda, F.J. Gotor, J. Malek, N. Koga, J. Therm. Anal. Calorim. 72 (2003) 901–906.
[18] J. Malek, Thermochim. Acta 355 (2000) 239–253.
[19] A. Rotaru, B. Jurca, A. Moanta, I. Salageanu, E. Segal, Rev. Roum. Chim. 51 (2006) 373–378.
[20] A. Rotaru, A. Kropidlowska, A. Moanta, P. Rotaru, E. Segal, J. Therm. Anal. Calorim. 92 (2008) 233–238.
[21] A. Rotaru, A. Mandruleanu, A. Moanta, P. Rotaru, E. Segal, J. Therm. Anal. Calorim. submitted for publication.
[22] C. Ozdilek, L. Toppare, Y. Yagci, J. Hacaloglu, J. Anal. Appl. Pyrol. 64 (2002) 363–378.
[23] A. Rotaru, A. Moanta, G. Popa, P. Rotaru, E. Segal, J. Therm. Anal. Calorim. in press.
[24] P. Budrugeac, Polym. Degrad. Stab. 89 (2005) 265–273.
[25] S. Vyazovkin, A.I. Lesnikovich, Thermochim. Acta 165 (1990) 273–280.
[26] S. Vyazovkin, Int. J. Chem. Kinet. 28 (1996) 95–101.
[27] J.W. Huang, C.C. Chang, C.C. Kang, M.Y. Yeh, Thermochim. Acta 468 (2008) 66–74.
[28] D.M. Minic, B. Adnadevic, Thermochim. Acta 474 (2008) 41–46.
[29] X.M. Cao, H. Li, X. Yang, Y. Duan, Y.W. Liu, C.X. Wang, Thermochim. Acta 467 (2008) 99–106.
[30] X. Ramis, J.M. Morancho, A. Cadenato, J.M. Salla, X. Fernandes-Francos, Thermochim. Acta 463 (2007) 81–86.
[31] A.A. Joraid, Thermochim. Acta 456 (2007) 1–6.
[32] H.E. Kissinger, Anal. Chem. 29 (1957) 1702–1706.
[33] T. Akahira, T. Sunose, Res. Rep. Chiba Inst. Technol. 16 (1971) 22–31.
[34] J.H. Flynn, L.A. Wall, J. Res. Natl. Stand. Bur. A: Phys. Chem. 70 (1966) 487–523.
[35] T. Ozawa, Bull. Chem. Soc. Jpn. 38 (1965) 1881–1886.
[36] J.M. Criado, J. Morales, Thermochim. Acta 16 (1976) 382–387.
[37] A.W. Coats, J.P. Redfern, Nature 201 (1964) 68–69.
[38] A.I. Lesnikovich, S.V. Levchik, J. Therm. Anal. 30 (1985) 237–262.
[39] P. Budrugeac, J. Therm. Anal. Calorim. 89 (2007) 143–151.
[40] P. Budrugeac, E. Segal, J. Therm. Anal. Calorim. 88 (2007) 703–707.
[41] S. Vyazovkin, A.I. Lesnikovich, Termochim. Acta 128 (1988) 297–300.
[42] A. Pratap, T.L.S. Rao, K.N. Lad, H.D. Dhurandhar, J. Therm. Anal. Calorim. 89 (2007) 399–405.
[43] A. Rotaru, A. Moanta, P. Rotaru, E. Segal, J. Therm. Anal. Calorim. 95 (2009) 161–166.
[44] M. Erceg, T. Kovacic, I. Klaric, Thermochim. Acta 476 (2008) 44–55.
[45] A. Kropidlowska, A. Rotaru, M. Strankowski, B. Becker, E. Segal, J. Therm. Anal. Calorim. 91 (2008) 903–909.
[46] P. Svadalk, Z. Zmrhalova, P. Pustkova, J. Malek, L.A. Perez-Maqueda, J.M. Criado, J. Non-Cryst. Solids 354 (2007) 3354–3361.
[47] B. Jankovic, B. Adnadevic, S. Mentus, Chem. Eng. Sci. 63 (2008) 567–575.
[48] S. Tiptipakorn, S. Damrongsakkul, S. Ando, K. Hemvichian, S. Rimdusit, Polym. Degrad. Stab. 92 (2007) 1265–1278.
[49] J. Šesták, G. Berggren, Thermochim. Acta 3 (1971) 1–12.